Est. 1984

ORIENTAL JOURNAL OF CHEMISTRY
An International Open Access, Peer Reviewed Research Journal

www.orientjchem.org

ISSN: 0970-020 X
CODEN: OJCHEG
2022, Vol. 38, No.(1):
Pg. 163-171

Synthesis, Cytotoxicity, Molecular Docking, Molecular Simulation and ADME Properties of Cinnamoylated Chloroquine Hybrid Analogues as Corona Virus Protease Inhibitors

K. R. JAYANTHI, K. HEMAPRIYA and SUBBAN RAVI*

Department of Chemistry Karpagam Academy of higher Education, Coimbatore-21, India.
*Corresponding author E-mail:ravisubban@rediffmail.com

http://dx.doi.org/10.13005/ojc/380120

(Received: October 20, 2021; Accepted: January 11, 2022)

ABSTRACT

In an attempt to challenge COVID-19, molecular docking of cinnamoylated chloroquine compounds **1–15** against main protease (Mpro) enzyme of SARS-CoV-2 was undertaken. To study the stability of the complex formed between the drug and the receptor, suitable docking possesses were selected and put into molecular dynamics studies. Further ADME properties were determined using SWISS ADME software. In the docking studies compounds **5, 9, 14 and 15** exhibited encouragable binding with the Mpro crystal structure with docking scores of -8.1, -7.9, -7.8 and -7.9 Kcal/mole respectively. It was observed that CYS145 and GLU166 played a significant role during the interaction of molecules with the active site of COVID-19 Mpro. Among compounds **5, 9, 14 and 15,** compound 5 had stable interactions with the protein, which might be the reason for the optimum RMSD, RMSF, radius of gyration and protein–ligand contacts (hydrogen bonding) values. The compound **5** was synthesised and tested for its cytotoxic activity against fibroblast L929 cell line. The above study indicated that the compound **5** as a promising agent, and during the drug discovery process it could be taken as a starting point for lead optimization.

Keywords: COVID-19, SARS-CoV-2, Docking studies, ADME properties, Cytotoxic activity.

INTRODUCTION

Corona virus from the family coronaviridae belongs to the order nidovirales and are mostly found to be distributed in human beings[1]. Once SARS-CoV-2 infects a cell, the host cell activities are totally controlled by the virus and its RNA gets translated to proteins with long chains, and in turn generate multiple copies. The viral proteases convert the long viral proteins into smaller pieces and activate them, and thereby play a critical role in the viral propagation. To treat the viral diseases like hepatitis C and HIV[2] FDA has approved a good number of viral protease inhibitors (like darunavir, atazanavir, boceprevir, etc.) as drugs for viral diseases. The protease reported from SARS-CoV2 is a protein having the shape of an heart and comprises of dimers of two identical subunits. When the molecules bind to specific sites[3] the protease activity is triggered.

In an attempt to challenge COVID-19, an in silico study was made and in this regard virtual screening of 15 cinnamoylated chloroquine hybrid analogues **(1-15)** against the crystal structure of the protease protein also known as 3CL hydrolase (Mpro) (PDB ID: 6Y2F) was carried out. This study aims to find an effective viral protease inhibitor and carried out the molecular docking study and also predicted ADME properties of these compounds **1-15**. Among these molecules, compound **5** with the least score in molecular docking studies and with a favourable ADME property and later it was subjected to further studies like molecular dynamics simulation to investigate the stability of the complex formed. Further the compound was synthesised and subjected to *In vitro* cytotoxic activity against fibroblast L929 cell line.

MATERIALS AND METHOD

Selection of drug target and Ligands

Cinnamoylated chloroquine hybrid analogues **1–15** were taken as the ligands and the protease protein with PDB ID: 6Y2F as the target protein for the in-silico studies. The X-ray crystal structure of the above protein complexed with a $\propto$ -ketoamide inhibitor was retrieved from the protein database.

Protocol for molecular docking studies

The Auto Dock 4.2 software package was used to carry out the docking. The ligands **1–15** were drawn and energy minimization of ligands were performed using a tool, known as Avogadro. Auto Dock and MGL tools were used for protein and ligand preparation and files which gives the output were saved in. pdbqt formats. After docking, the ligand–protein binding interaction was analysed using Discovery Studio 3.5, UCSF Chimera 1.13.1 and PyMOL 2.3. The binding energy was estimated with Mpro (PDB ID: 6Y2F) at resolution 1.95 Å. All the water molecules were removed in addition to the deletion of heteroatoms and co-crystal ligand from 6Y2F and then MGL tool was used to add Gasteiger charges and H- atoms and these are stored in. pdbqt format. The grid box dimension along x, y, and z axis was fixed at 40 × 40 × 40 Å, with 0.375 Å spacing. All the input files, were made by Auto Dock graphical user interface. Lamarckian GA (4.2) and a genetic algorithm were used for docking simulation and evaluation. The Auto Dock tool was used to analyse the ligand-receptor interactions in their best binding poses and the lowest Gibbs free binding energy (estimated as ΔG in kcal/mol) conformers were selected for post-dock analysis.

Molecular dynamic simulations

The structure of the complex obtained from the protein 6Y2F and compound **5** was made ready for MD simulation. GROMACS-2021 version was employed to carry out 50 ns simulations using the CHARMM36 force field. For solvating the complexes, the SPCE water model was chosen followed by addition of ions to neutralize. Minimization of energy was performed with a tolerance of 1000 kJ/mol/nm. System equilibration was carried out for 50 ns using NVT and NPT ensemble. The NPT ensemble (T = 300 K and P = 1 bar) was carried out and the results of the protein-ligand complexes were analysed.

ADMET properties

Using the Swiss ADME software the various physicochemical and ADMET-related in silico properties were predicted.

Synthesis of compound 5

Preparation of compound (A)

4,7-dichloroquinoline (100 g) and 200 mL of ethylenediamine were taken in a RB flask and maintained at 110ºC with continued stirring 24 hours. Once the reaction is completed, the contents in the flask was transferred into a container with cold water; the content was continuously stirred for 120 min to yield a solid and then filtered. Then petroleum ether was used to wash the yielded solid and by means of a vacuum tray dryer the product was dried at 40ºC (106 g, yield 97.4%).

Synthesis of compound B

The 4-chloro benzaldehyde (1.0 g, 1.0eq) was taken in a 100.0 mL RB flask having 14.5 mL dimethylformide (DMF) and malonic acid (1.09 eq) and added with Diaza bicyclooctane (DABCO 1.1eq) which was used as a catalyst. The reaction mixture was heated to 110^{0}C and at the same temperature and retained for 2.0 hour. TLC was used to determine the Completion of the reaction. The reacted contents were poured into 50.0 mL water maintained at 5ºC and using ethyl acetate 2 x 25 mL the product was extracted. Using anhydrous Na_2SO_4 the ethyl acetate layer was dried, concentrated and the yielded solid was thoroughly washed with petroleum ether (10.0 mL), and vacuum dried at 45ºC to yield B (3-(4-chloro phenyl) acrylic acid).

Compound B

Colour: White solid; Yield: 68.4%, IR (cm^{-1}, KBr,): 3432, 3018, 1631, 1532, 1425, 1221, 776; ^1H NMR (Deuterated acetone, 400 MHz) δ:7.69 (2H, d, J = 8.1Hz), 7.56 (1H, d, J = 15.9Hz,), 7.37 (2H, d, J = 8.1Hz), 6.45 (1H, d, J = 15.9Hz); MS: ESI positive mode (m/z):182 $[M+H]^+$.

To compound B (1.0eq) was dissolved in 20 mL of THF and it was maintained at 0^0C, then added 1.2 eq of dicyclo hexyl dicarbodimide (DCC), stirred for 20 mintue. Then added 1.2eq of N-hydroxy benzo triazine (HOBT), stirred for 40 min and to this a solution of compound-A (1.2 eq) was added dropwise at 0ºC for 80 minute. The reaction mixture was kept overnight at 20-27ºC and monitored by TLC. Once the reaction gets completed the mass was poured in to 50 mL cold water and extracted with chloroform 3 x 30 mL. The chloroform layer was dried, concentrated under vacuum, added with 20 mL THF and kept at 0ºC for 24 hours. The yielded solid was filtered, vacuum dried at 50ºC for 4 h to get compound **5**

Compound 5: N-(2-(7-chloroquinolin-4-ylamino) ethyl)-3-(4-chlorophenyl) acrylamide

Colour: White solid; Yield: 55.0%, ^{1}HNMR ($CD_3OD + CDCl_3$, 400MHz) δ : 8.41 (1H, d, J = 5.56), 7.87(1H, d, J = 8.32), 7.67(1H, d, J = 2.14), 7.44 (1H, d, J = 15.71), 7.39 (2H, d, J = 8.32), 7.29 (1H, dd, J = 2.21, 7.89), 7.29 (2H, d, J = 8.38), 6.54-6.39 (2H, m,), 3.69-3.65 (2H, m,), 3.53-3.49 (2H, m). MS : ESI positive mode (m/z) 386.4 $[M+H]^+$ and Anal. Calcd. for $C_{20}H_{17}Cl_2N_3O$: C,62.18; H, 4.43; N, 10.87; Found: C,62.19; H, 4.45; N, 10.83.

***In vitro* cytotoxic activity of compound 5**

From National Centre for Cell Sciences, Pune, India, the Fibroblast L929 cell was procured and was cultured in a dedicated flask with Dulbecco's modified Eagles medium. It was added with 10% FBS, sodium bicarbonate, L-glutamine and antibiotic solutions as supplements.

This was kept at 37ºC in an incubator (NBS Eppendorf, Germany) humidified with 5% CO_2. Inverted phase contrast microscope was used to evaluate the viability of cells. MTT assay was used to evaluate the cytotoxic activity.

Cytotoxicity Evaluation

The confluent cells containing approximately 5 x 10^3 cells/well was suspended in 96 well plates and allowed to grow in the incubator for 24 hours. Then the growth medium was removed and 100 μL of fresh solution of compound 5 in DMEM in various concentration (100 μg, 50 μg, 25 μg, 12.5 μg, 6.25 μg in 500 μL of DMEM) were added and allowed to grow in the same condition. The cells not treated with any one the compounds act as control and was maintained in the same environment.

Cytotoxicity Assay by Direct Microscopic observation

After one full day of treatment the plate was investigated through a microscope (Olympus CKX41) and the images were recorded. If any remarkable changes are detected with respect to the cell morphology, like vacuolization of cells, rounding of cells, shrinking of cells, and presence of granulation in the cytoplasm of the cells then they cytotoxicity is indicated.

Cytotoxicity by MTT Assay

After 24 h, from the wells the sample content was removed and MTT solution of about 30 μL was added, well mixed and kept for another 240 minute. at 37ºC in the same incubator (Laura B. Talarico *et al.,* 2004). After that, the supernatant was removed and the resulted formazan crystals were dissolved in 100 μL of DMSO (Sigma Aldrich, USA) and absorbance values were measured at 540 nm. The viability percentage was determined using the formula, the ratio between the mean OD of the sample x 100 to the mean OD of control. The observed results are exhibited in the Table 1. For the compound 5 the LC_{50} value was determined as 214.092 μg/mL. This shows that the compound was not cytotoxic in nature.

Table 1: The optical density values obtained for the compound 5 by MTT assay

Sample Concentration (μg/mL)	OD value I	OD value II	OD value III	Average OD	Percentage Viability
6.25	0.6731	0.6727	0.6763	0.6740	98.54
12.5	0.6325	0.6315	0.6328	0.6323	92.44
25	0.6156	0.6194	0.6117	0.6156	90.00
50	0.5531	0.5555	0.5634	0.5573	81.48
100	0.5221	0.5285	0.5227	0.5244	76.67
Control	0.6864	0.6839	0.6817	0.6840	100.00

RESULTS AND DISCUSSION

It is widely discussed in the literature that chloroquine (CQ) and hydroxychloroquine (HCQ) are FDA approved drugs for malaria and autoimmune diseases and they increase the endosomal pH to inhibit viral infections[4-7]. Earlier in our laboratory a series of novel hybrid molecules of cinnamoylated chloroquines were evaluated for malaria[8]. From this series15 compounds (Fig. 1) **1–15** were taken for the present study. One of our objective of taking up of this work with these selected molecules **1-15** is to find out where these molecules bind inside the Mpro binding site and in turn it might help us to consider them as a probable template which can be used further for the development of new Mpro viral infection inhibitors.

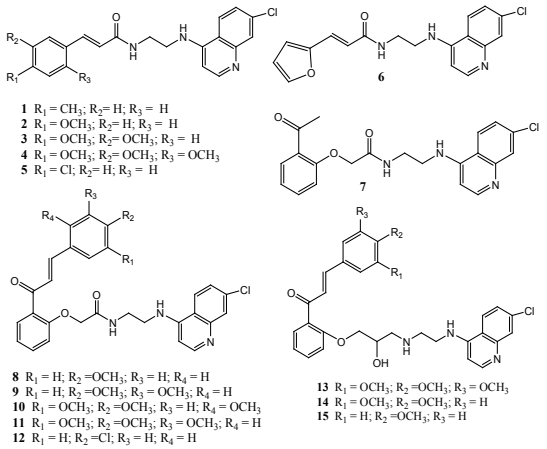

Fig. 1. Cinnamoylated chloroquine hybrid compounds with antimalarial activity

The molecular docking and binding energy estimation were carried out for the above 15 compounds with the documented structure of the viral protein Mpro (PDB ID: 6Y2F) at 1.95 Å resolution. With a positive control the optimised docking protocol was validated. The Co-crystal ligand was docked once again into the catalytic binding site of 6Y2F using the Auto Dock tool. Also using the PyMol application the RMSD value was determined between the docking and co-crystal ligand poses. The docking protocol was validated by obtaining a low RMSD value (<1.2). Conformers with lowest energy has been carried forward for the post-docking analysis The results were presented in the Table 2.

Table 2: Docking scores (Kcal/mole) for the compounds 1-15 using Auto dock

Compound	Binding score	Compound	Binding score
1	-7.5	9	-7.9
2	-7.3	10	-6.7
3	-7.2	11	-6.9
4	-7.3	12	-6.6
5	-8.1	13	-7.3
6	-6.8	14	-7.8
7	-6.5	15	-7.9
8	-7.5		

The 6Y2F structure consists of two protomers identical with each other and it is a homodimer composite. There are three domains in each monomer. Domain I is made up of the amino acid residues 8–101, and this was followed by domain II which is made up of residues 102–184. The domain III is in the form of a globular cluster and consists of five α-helices and this arrangement controls the protein dimerization. A cleft and a chymotrypsin fold are formed in between the domain I and II and they act as a substrate binding pocket. A long-extended loop connects domain II and III and consists of residues 185–200. In addition to this an extra domain is also present which consists of residues in the C-terminal. The active site amino acid residues which are present in the I and II domains are further divided in to subsites S1–S6, and these sites act as substrate binding pockets for the inhibitors.

In the S1 subsite the residues His41–Cys145 collectively called as the catalytic dyad is present and the subsites S2 and S4 consists of hydrophobic side chains. During proteolysis in order to stabilise the transition process the residues CYS145, SER144, and GLY143 interact with a conserved GLN carboxylate anion present in the cleavage site and forms an oxyanion hole which is an essential function of the S1 subsite[9,10]. In the present study, the binding mode analysis of compounds **1–15** with Mpro exhibited favourable hydrogen bonding interactions along with alkyl and mixed π-alkyl hydrophobic interactions at the active binding pocket, as shown in **Fig. 2**-**5**. Among the compounds docked compound **5, 9, 14** and **15** showed good scores and interactions. Rather than one Among the compounds docked compound **5**, **9, 14** and **15** showed good scores and interaction. Rather than one hydrogen-bonding interaction, it is always advantageous to have multiple hydrogen-

bonded interactions with the catalytic centre (S1 subsite) of the target proteases[9,10].

The amine hydrogen of the compound **5** (Fig. 2) showed a tri-center H- bond interaction to the oxygen of His A: 164 (2.87 A) and Cys A: 145 (2.27 A) and was found to be present firmly and deeply in the S1 pocket of the protease. The NH hydrogen of ARG A: 188 formed an H-bond with the amide carbonyl oxygen of **5**. Further the π electrons of the quinolone moiety and the chloro substituted benzene ring showed hydrophobic Pi-alkyl interaction with CYS A:145 and PRO A:168 respectively. Van der Waals interactions were observed with MET A 165, GLU A:166, HIS A:41, MET A:49, GLY A:143 and THR A:190.

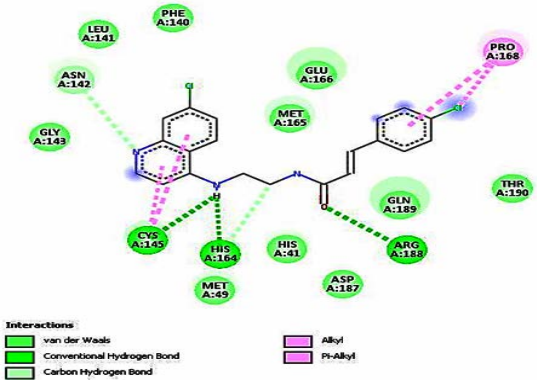

Fig. 2. Interactions of compound 5with the protein PDB ID:6Y2F

Similarly compound **9** (Fig. 3) was also found to be seated in the S1 pocket of the protease and nitrogen atom of the quinolone moiety formed a hydrogen bond interaction to the oxygen of Cys A:145 (2.86 A) and further the amide NH formed an hydrogen bond with C=O of GLU A:166 (2.29 A). Further the π electrons of the aromatic ring showed hydrophobic Pi-alkyl interaction with MET A 165 and PRO A:168. Van der Waals interactions were observed with, MET A:49, HIS A:169, GLN A:142 and THR A:190.

In the compound **14** (Fig. 4) the hydroxy hydrogen formed a tri-center hydrogen bonded interaction to the oxygen of Cys A:145 (2.29 A) and SER A:144 (2.87 A) and LEU A:141(2.96 A). Further the π electrons of the quinoline moiety and they showed hydrophobic Pi-alkyl interaction with HIS A:41 and MET A:165. Van der Waals interactions were observed with GLU A:166, HIS A:164, ARG A:188, GLY A:143 and THR A:190.

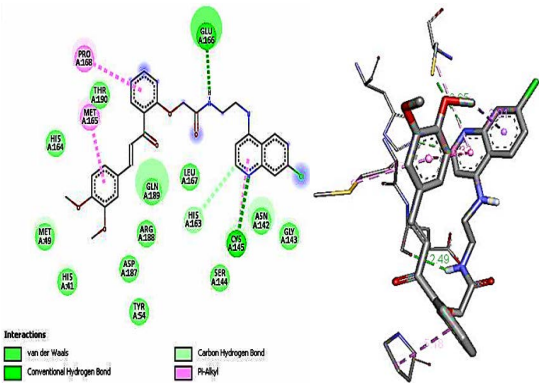

Fig. 3. Interactions of compound 9with the protein PDB ID:6Y2F

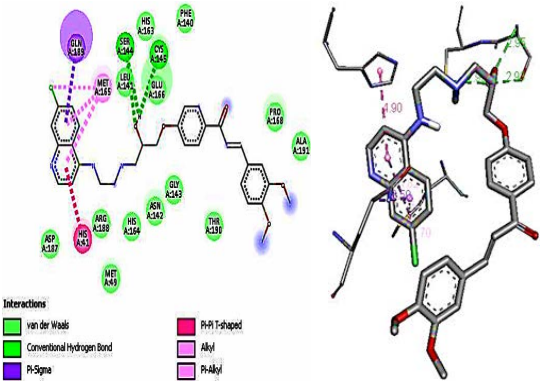

Fig. 4. Interactions of compound 14 with the protein PDB ID:6Y2F

More interestingly in the compound **15** (Fig. 5) the hydroxy hydrogen exhibited tri-center hydrogen bond interaction to the oxygen of Cys A: 145 (2.27 A), ASN A:142 (2.75 A), SER A:144 (2.60 A) and GLY A 143(2.87 A). Further the π electrons of the quinoline moiety showed hydrophobic Pi-alkyl interaction with HIS A:141, and MET A 165. Van der Waals interactions were observed with, GLU A:166, HIS A:164, MET A:49, ARG A:188 and THR A:190.

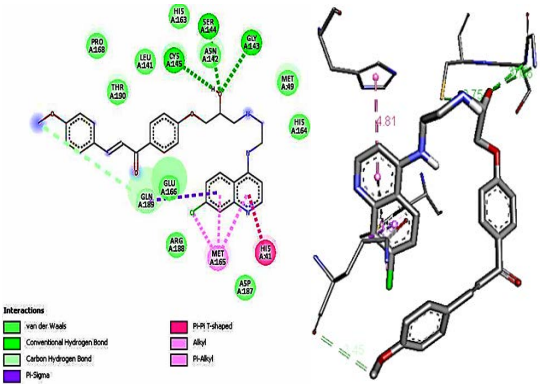

Fig. 5. Interactions of compound 15 with the protein PDB ID:6Y2F

In compound **9**, the amide NH formed an hydrogen bond with GLU A:166 (2.29 A). It was reported that GLU 166 has a significant role in the dimerization of two protomers and also it helps in the shaping of S1 pocket of the substrate-binding site[49]. Due to this reason compound **9** can effectively inhibit the functions of 6Y2F. With respect to other ligands, they showed H-bonded interaction either with CYS145 and/or HIS41 residues of the active pocket's catalytic domain, which suggests that these two amino acids plays a critical role for inducing Mpro inhibitory activity.

Molecular dynamics (MD) simulations studies of compound 5 with 6Y2F

Based on the interactions made by the compounds **5, 9, 14** and **15** in the binding site and the respective binding energy determined (Fig. 2-5, Table 1), we have chosen the docked complex of compound **5** to run Molecular Dynamics (MD) simulation. Evaluation ws made based on the stability criteria during the MD simulation study using GROMACS 2021 package. To validate, confirm, and study the time-dependent interactions of ligand **5** with 6Y2F and the stability of the complex formed between the ligand and the receptor, simulation was carried out for 50ns, and the dynamic stability of the complex was studied using the characteristics like protein–ligand RMSD, L-RMSF, radius of gyration and protein–ligand contacts (hydrogen bonding). The study revealed that during the simulation period the energy value of compound **5** was consistent and indicates that the Compound 5 possess the required stable structure for the drug designing processes.

Analysis of root mean square deviations of protein (RMSD)

RMSD analysis was carriedout to investigate the conformational stability of the ligand-protein complex formed between compound **5** and the protein 6Y2F and to study the conformational stability of the protein 6Y2F backbone. It is investigated to find out whether there is any movement of atoms in the protein 6Y2F when it is bound with the compound 5 in its active sites. RMSD plot score was calculated for 50 ns. The average backbone RMSD for unbound and bound complex (between compound **5** and 6Y2F) varied between 0.1–0.22 nm and found to be stable for the entire 50 ns for which MD simulation was carried out.

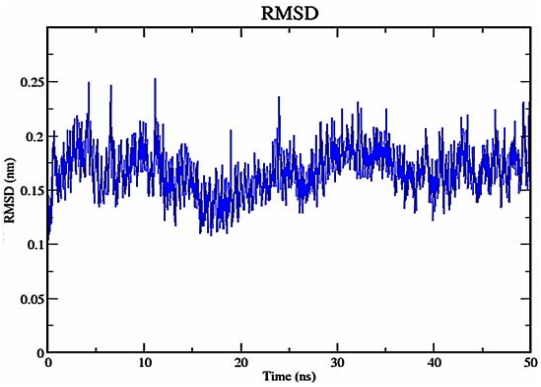

Fig. 6. RMSD of solvated SARS-CoV-2 M pro protein backbone and in complex with ligand 5 during 50ns molecular dynamics simulation

Protein root mean square fluctuation (RMSF)

The structural integrity of both Mpro ligand complex and the protein backbone were predicted by calculating the RMSF value. This also helps to determine the binding stability of the protein with the ligand throughout the period of simulation. The results of the RMSF calculations made for the MPro ligand complex and for the protein were presented in the form of a graph in Fig. 7. Each and every peak in this graph, represents the protein area that fluctuates to a larger extent during the period of simulation. Usually the N-terminal and C-terminals, the so called 'tails' fluctuate to a greater extent when compared with other residues present in the protein. The average RMSF value obtained for the protein and the protein complex formed between the protein and the compound 5 was 0.15nm. The result suggested that compound 5 binding with the protein 6Y2F substantially decreased the RMSF values.

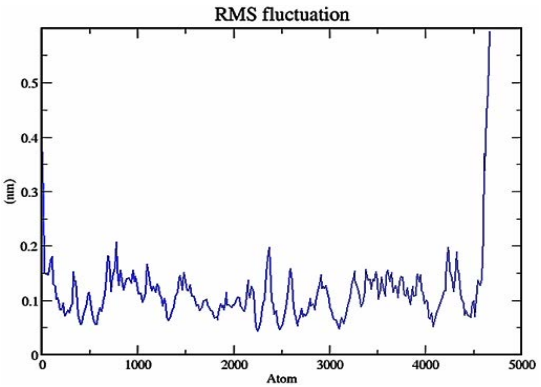

Fig. 7. RMSF values of solvated SARS-CoV-2 M pro protein and in complex with ligand 5 plotted against residue numbers

Protein–ligand contacts

The investigation of interactions taking place between the protein and the ligand (compound **5**) more important as it gives the information about the specific target sites. During molecular docking analysis of compound **5** it (Fig. 2) was firmly placed inside the S1 pocket of 6Y2F protein and amine hydrogen exhibited hydrogen bonds with the oxygen of Cys A:145 (2.27 A) and His A:164 (2.87 A). Further the amide carbonyl oxygen formed an hydrogen bond with NH hydrogen of ARG A:188 (3.24 A). In the MD simulation study, the interactions existed between the compound **5** and 6Y2F were found stable over the simulation period (Figure 8, 9).

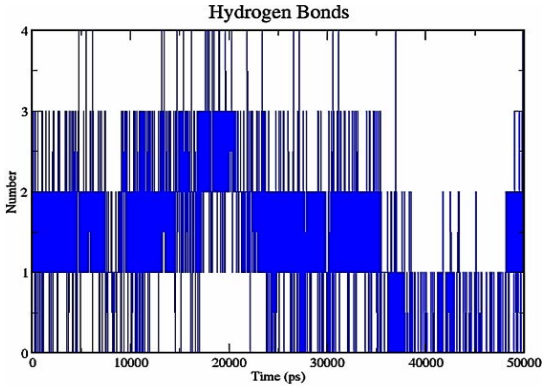

Fig. 8. Plot of number of hydrogen bond formation within the SARS-CoV-2 M pro protein complex with ligand 5

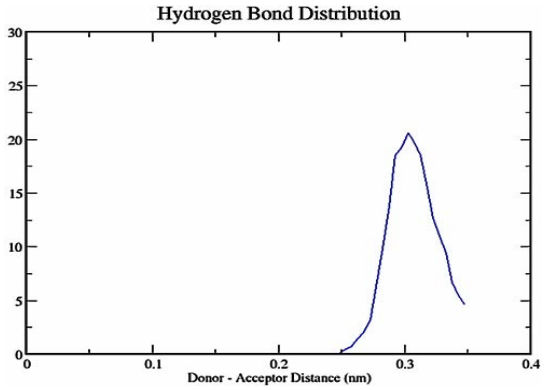

Fig. 9. Plot of hydrogen bond distribution within the SARS-CoV-2 M pro protein, SARS-CoV-2 Mpro protein complex with ligand 5

Radius of gyration (Rg)

Radius of gyration (Rg) is a, important parameter used to assess the folding of a protein from its regular secondary structure into its three dimensional structure. Rg is used not only to identify any change is there in protein structure compactness but also gives information about its overall dimension. During binding of compound **5**, initially (upto 30ns) the Rg value was 2.15nm for both ligand bound and unbound protein and latter from 30ns and 50ns of simulation the value was 2.2. This suggests that the secondary structure of the protein was not disturbed during binding of the compound **5** throughout the simulation period. The result strongly indicate that tight packing of the protein was observed even after binding of the ligand and thus making a stable complex (Figure 10).

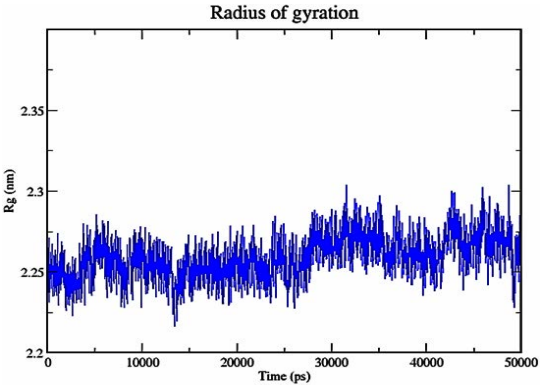

Fig. 10. Rg during 50ns molecular dynamics simulation of SARS-CoV-2 M pro protein and in complex with ligand 5

In Silico ADME properties of selected ligands 5, 9, 14 and 15

Table 2 exhibits the results of the ADME characteristics (absorption, distribution, metabolism, and excretion) determined using Swiss ADME package. Through this study the physicochemical properties of the compounds, their biological functions and the drug likeness of a compound could be determined. These properties like solubility, ionization (pKa), permeability, lipophilicity, transporters, and pharmacokinetic parameters are used to predict the efficacy of the compounds **5, 9, 14** and **15**. The results are presented in Table 3. It was observed from the table with respect to the pharmacokinetics properties that compounds **5, 9, 14** and **15** qualifies the drug likeness criteria. No violations of Lipinski's rule of five was observed.

Synthesis of compound 5

4,7-dichloroquinoline reacted with ethylenediamine at 110ºC under stirring for 24 h to yield an intermediate compound A. Also 4-chloro benzaldehyde reacted with malonic acid in presence of a catalyst Diaza bicyclooctane (DABCO) to yield another intermediate B. Compound A and B react with each other in presence of dicyclohexyl dicarbodimide (DCC) to form the compound **5** (Scheme 1).

Table 3: Below table shows the ADME properties of compounds 5, 9, 14 and 15 determined using Swiss ADME

Table 3a: Physicochemical parameters of compounds 5, 9, 14 and 15

Molecule	Vina Score Kcal/mol	MW	No. Heavy atoms	No. Rotatable bonds	No. H-bond acceptors	No. H-bond donors	MR	TPSA
5	-7.4	386.27	26	7	2	2	108.1	54.02
9	-7.9	546.01	39	13	6	2	152.28	98.78
14	-6.6	562.06	40	14	7	3	158.05	101.94
15	-7.4	532.03	38	13	6	3	151.56	92.71

Table 3b: Solubility parameters of compounds 5, 9, 14 and 15

Molecule	iLOGP	iLOGP	XLOGP3	WLOGP	MLOGP	Ali Log S	Bioavailability Score
5	3.26	3.26	5.44	4.48	3.31	-6.33	0.55
9	4.1	4.1	5.53	5.11	2.15	-7.36	0.55
14	4.95	4.95	5.13	4.94	2	-7.02	0.55
15	4.42	4.42	5.16	4.93	2.34	-6.85	0.55

Table 3c: Pharmacokinetic parameters of compounds 5, 9, 14 and 15

Molecule	GI absorption	BBB permeant	Pgp substrate	CYP1A2 inhibitor	CYP2C19 inhibitor	CYP2C9 inhibitor	CYP2D6 inhibitor
5	High	Yes	No	Yes	Yes	Yes	Yes
9	High	No	Yes	No	Yes	Yes	Yes
14	High	No	Yes	Yes	Yes	Yes	No
15	High	No	Yes	Yes	Yes	Yes	Yes

Table 3d: Drug likeliness rules of compounds 5, 9, 14 and 15

Molecule	Lipinski rule, No. of violations	Ghose rule, No. violations	Veber rule, No. of violations	Egan rule No. of violations	Muegge rule, No. of violations
5	0	0	0	0	1
9	1	2	1	0	1
14	1	3	1	0	1
15	1	2	1	0	1

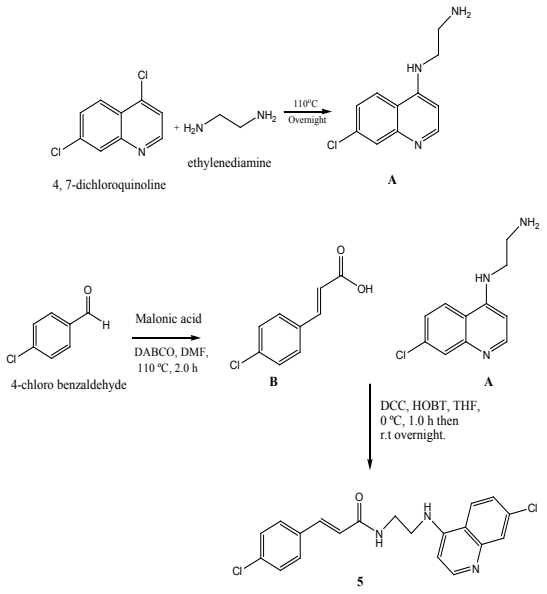

Scheme 1. Synthesis of compound 5

Cytotoxic activity of compound 5

The concept behind the *In vitro* cytotoxicity test is that toxic compounds could affect the primary functions of cells which are present in common in all the tissues leading to determinable cellular structural and functional damage. The fibroblast cells are highly proliferative and are present in all types of connective tissues. In cytotoxicity evaluation with respect to cellular viability and proliferation, normally fibroblast cells are used. In this aspect, cytotoxicity testing with the cultures having fibroblast cell is considered as general bioassay, which provides appropriate information regarding basal cytotoxicity[11]. The cytotoxicity of the compound **5** was determined by MTT assay against fibroblast L929 cell lines. It behaved in a dose- and time-dependent manner. The LC_{50} value of the compound was calculated and the value obtained for the compound **5** is 214.092 μg/mL. This shows that the compound was not cytotoxic in

nature. The above data was complemented by the in-silico study and indicated that the compound **5** is a promising agent, and might act as a starting point for lead optimization in drug discovery.

CONCLUSION

The main protease (Mpro) enzyme of SARS-CoV-2 is an attractive drug target for antiviral drug design. In this aspect, molecular docking studies, molecular dynamics studies and predicted ADME properties was carried out for compounds **1-15**. In the docking studies compounds **5, 9, 14** and **15** exhibited encouraging results the crystal structure of Mpro over the other selected molecules in this study with docking scores of -8.1, -7.9, -7.8 and -7.9 Kcal/mole respectively. The molecules interacted with CYS145 and GLU166 amino acids present in the active site of COVID-19 Mpro. Among compounds **5, 9, 14** and **15**, compound **5** showed stable interactions with the protein and gave optimum RMSD, RMSF, radius of gyration and protein–ligand contacts (hydrogen bonding) values. Most of the analogs from **1-15** showed acceptable ADMET properties, with respect to GI absorption, P-gp interaction, and low toxicity. The compound **5** was synthesised and tested for its cytotoxic activity against fibroblast L929 cell line which showed a LC_{50} value of 214.092 μg/mL. The above data suggested that the compound **5** is a promising agent, that might act as a beginning point for optimization in drug discovery.

ACKNOWLEDGMENT

The authors are thankful to Karpagam Academy of Higher Education Central Instrumentation Facility for providing facilities to characterise the compounds.

Conflict of Interest

The authors have no conflict of interest.

REFERENCES

1. Richman, D. D.; Whitley, R. J.; Hayden, F. G. *Clinical Virology*., **2016**, *4*, 978-1-683-67316-3.
2. Himanshu, R.; Atanu, B.; Yash P. S.; Akhil, S.; Lovejit, S.; Gourav, S.; Usha, Y. N.; Vikash, K. D.; Gyan, M. *Mol Divers*., **2021**, *25*, 1905–1927.
3. Choudhary, M. I.; Shaikh, M.; Wahab, A.; Rahman, A.; *Agency for Healthcare Research and Quality*., **2020**, *15*(7), 0235030.
4. Devaux, C. A.; Rolain, J. M.; Colson, P.; Raoult, D. *Int J Antimicrobl Agents*., **2020**, *55*(5), 105938.
5. Touret, F.; Lamballerie, X. *Antiviral Res*., **2020**, *177*, 104762.
6. Wang, X.; Cao, R.; Zhang, H.; Liu, J.; Xu, M.; Hu, H.; Li, Y.; Zhao, L.; Li, W.; Sun, X.; Yang, X.; Shi, Z.; Deng, F.; Hu, Z.; Zhong, W.; Wang, M.; *Cell Discovery.,* **2020**, *6*(28), 1-5.
7. Alim, A. B. *Pharmacol. Res. Perspect*., **2017**, *5*(1), 1-13.
8. Gayam, V.; Ravi, S. *Eur. J. Med. Chem*., **2017**, *135*, 382-391.
9. Marwa, A. A.; Fayed, E.; Inas, A.; Abdallah, M.; Hanan, E.; Ahmed, M.; Yassmin, M.; Khaled, A. M.; Abouzid, Y.; Elshaier, A. M. M.; *Arab. J. Chem*., **2021**, *14*, 103092.
10. Seketoulie, K.; Swapnil, P.; Seung, J. C.; *Sci. Rep*., **2020**, *10*, 17716.
11. Freshney, R. I. *J. Chem. Technol. Biotechnol.,* **2000**, *45*(4), 330.